

# Coordination of Graphene Oxide with Fe<sub>3</sub>O<sub>4</sub> Nanoparticles and Its Enhanced Optical Limiting Property

Xiaoyan Zhang<sup>1</sup>, Xiaoying Yang<sup>2</sup>, Yanfeng Ma<sup>1</sup>,  
Yi Huang<sup>1</sup>, and Yongsheng Chen<sup>1,\*</sup>

<sup>1</sup>Key Laboratory of Functional Polymer Materials and Center for Nanoscale Science and Technology, Institute of Polymer Chemistry, College of Chemistry, Nankai University, Tianjin 300071, China

<sup>2</sup>School of Pharmaceutical Sciences, Tianjin Medical University, Tianjin 300070, China

A graphene oxide–Fe<sub>3</sub>O<sub>4</sub> (GO–Fe<sub>3</sub>O<sub>4</sub>) hybrid material was prepared by a simple chemical precipitation method. The formation of this hybrid material was verified by Fourier transform infrared spectroscopy, high resolution transmission electron microscopy and X-ray powder diffraction. The optical limiting performance of this hybrid material was studied using the Z-scan measurement, which shows a much enhanced optical limiting performance compared with GO and is comparable with the benchmark material-C<sub>60</sub>. The mechanism responsible for this enhancement may be attributed to the enhanced nonlinear scattering effect introduced by the Fe<sub>3</sub>O<sub>4</sub> nanoparticles.

**Keywords:** Graphene Oxide, Fe<sub>3</sub>O<sub>4</sub>, Optical Limiting.

## 1. INTRODUCTION

Graphene, a single carbon layer of the graphite structure, has received considerable attention for its excellent thermal,<sup>1</sup> mechanical,<sup>2</sup> and electrical<sup>3</sup> properties. Due to its semi-metallic nature and two-dimensional structure, graphene has found applications in many fields, such as field-effect transistors,<sup>4</sup> transparent anode,<sup>5</sup> sensor,<sup>6</sup> etc. Recently, graphene has emerged as a new class of material with potential optical applications, and its optical limiting (OL) properties have been investigated.<sup>6,7</sup> Liu et al.<sup>7</sup> used the water soluble oxidated graphene—graphene oxide (GO) as the OL material, and the results shows that two-photon absorption dominates nonlinear absorption process of GO in the case of picosecond pulses, while excited state nonlinearities play an important role in the case of nanosecond pulses. Xu et al.<sup>8</sup> prepared a graphene-porphyrin hybrid material, which shows much better OL property than the benchmark optical limiting material C<sub>60</sub> due to the photoinduced electron and/or energy transfer between the two species. This indicates that GO is an ideal material in OL devices. At the same time, metal nanoparticles<sup>9,10</sup> have been known to possess large OL properties and ultrafast response times. For example,

Singh et al.<sup>9</sup> investigated the OL property of iron oxide and found that nonlinear scattering was the dominant mechanism. Chin and coworkers<sup>10</sup> reported silver coated carbon nanotubes and found that the silver particles could contribute to the OL property of carbon nanotubes due to the enhancement of nonlinear scattering effect. In this paper, we prepared a Fe<sub>3</sub>O<sub>4</sub> modified GO hybrid material by a simple chemical precipitation method and investigated its OL property. As expected, GO–Fe<sub>3</sub>O<sub>4</sub> hybrid exhibits a much enhanced optical limiting performance compared with GO due to the enhanced nonlinear scattering.

## 2. EXPERIMENTAL DETAILS

### 2.1. Instruments and Measurements

Fourier transform infrared spectroscopy (FTIR) spectra were obtained on a BRUKER Tensor 27 spectrometer. The samples were homogeneous dispersed in KBr pellets. Transmission electron microscopy (TEM) images were obtained on a FEI TECNAI-20 instrument operated at 200 kV. X-ray powder diffraction was conducted on a D/Max-2500 instrument.

The open-aperture Z-scan experiments were performed with linearly polarized 5 ns pulses at 532 nm generated from a frequency doubled Q-switched Nd:YAG laser. The

\*Author to whom correspondence should be addressed.

spatial profiles of the pulses are of nearly Gaussian form after the spatial filter. The pulses are split into two parts: the reflected pulse was used as reference, and we focused the transmitted pulse onto the sample by using a 25-cm focal length lens. The input pulse energy was 80  $\mu$ J. The sample was placed at the focus where the spot radius of the pulses was about 30  $\mu$ m. The reflected and transmitted pulse energies were measured simultaneously with two energy detectors (Moletron J3S-10). C<sub>60</sub> was employed as a standard. To compare optical limiting effect, all of the sample concentrations were adjusted to have same linear transmittance of 75% at 532 nm in 5-mm-thick cells.

## 2.2. Materials

Graphite was purchased from Qingdao Tianhe Graphite Co. Ltd., with an average particle diameter of 4  $\mu$ m (99.95% purity). Ferric chloride hexahydrate (FeCl<sub>3</sub> · 6H<sub>2</sub>O), ferrous chloride tetrahydrate (FeCl<sub>2</sub> · 4H<sub>2</sub>O), sodium hydroxide were purchased from Tianjin No. 3 Chemical Plant. A dialysis chamber was purchased from Beijing Dingguo Biotechnology Co. (diameter = 36 mm), which had a molecular weight cutoff of 8000–15000 g mol<sup>-1</sup>.

## 2.3. Synthesis of Graphene Oxide (GO)

GO was prepared according to a modified hummers method.<sup>11</sup> The GO was confirmed to exist as individual sheets in solution.<sup>12</sup> The sizes of the GO sheet are mainly distributed between 200 and 500 nm determined by a statistical analysis using atomic force microscopy. In detail, graphite powder (5 g), NaNO<sub>3</sub> (3.75 g) and KMnO<sub>4</sub> (15 g) was vigorously stirred at room temperature for 5 days in concentrated H<sub>2</sub>SO<sub>4</sub> (375 ml). After that 5% H<sub>2</sub>SO<sub>4</sub> (1 L) aqueous solution was added to the reaction with the temperature kept at 98 °C for 2 h. Then the reaction was cooled to 60 °C. After 30% H<sub>2</sub>O<sub>2</sub> (30 ml) was added and the reaction was further stirred for another 2 h, the mixture was centrifuged to collect the bottom product and sequentially washed with 5% H<sub>2</sub>SO<sub>4</sub>/0.5% H<sub>2</sub>O<sub>2</sub> (10 times), 5% HCl solution (5 times), and then washed repeatedly with water until the pH of the supernatant was neutral. Finally the material was dried to obtain a loose brown powder.

## 2.4. Synthesis of GO–Fe<sub>3</sub>O<sub>4</sub> Hybrid via Chemical Deposition

GO–Fe<sub>3</sub>O<sub>4</sub> hybrid was prepared according to our previous method.<sup>13</sup> In short, GO (40 mg) was first sonicated in dilute NaOH aqueous solution (100 mL, pH = 12) for several hours to transform the carboxylic acid groups to carboxylate anions, followed by thorough dialysis until the dialysate became neutral. The resulting product was condensed to 20 mL and placed in a 50 mL round-bottom flask. The flask was then purged with N<sub>2</sub> for 30 min.

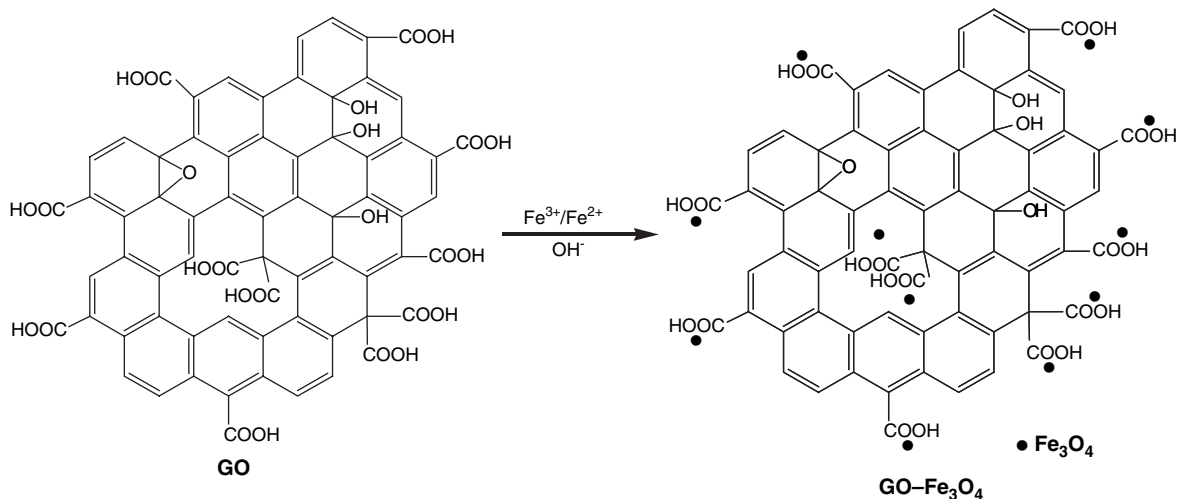
A solution of FeCl<sub>3</sub> · 6H<sub>2</sub>O (48.0 mg) and FeCl<sub>2</sub> · 4H<sub>2</sub>O (763.4 mg) in water (5 mL) was purged with N<sub>2</sub> for 30 min and then added to the above flask. The obtained mixture was stirred overnight under N<sub>2</sub> for ion exchange. After a thorough washing with water consisting of several centrifugation cycles under a N<sub>2</sub> atmosphere to remove excess iron salts, the solid product was redispersed in 25 mL water in a two-necked round bottom flask under a N<sub>2</sub> atmosphere. A NaOH aqueous solution (4 mL, 3 M) was added dropwise under N<sub>2</sub>. The mixture was kept stirring at 65 °C for a further 2 h. Then the mixture was washed thoroughly with water to neutral and dried under vacuum at room temperature.

## 3. RESULTS AND DISCUSSION

The GO–Fe<sub>3</sub>O<sub>4</sub> hybrid was prepared by chemical deposition of iron ions using water soluble GO as carriers (Scheme 1).<sup>13</sup> From the FTIR spectra of GO and GO–Fe<sub>3</sub>O<sub>4</sub> hybrid, the notable FTIR feature of GO corresponding to the carboxyl stretching at 1730 cm<sup>-1</sup> is shifted to 1600 cm<sup>-1</sup> in the spectra of GO–Fe<sub>3</sub>O<sub>4</sub> hybrid material. This could be attributed to the coordination interaction between the –COOH and Fe<sub>3</sub>O<sub>4</sub>. The characteristic peak corresponding to the stretching vibration of Fe–O bond is also shifted to higher wavenumbers of 702 cm<sup>-1</sup> compared with that of 570 cm<sup>-1</sup> reported for the stretching mode of Fe–O in bulk Fe<sub>3</sub>O<sub>4</sub>,<sup>14</sup> suggesting that Fe<sub>3</sub>O<sub>4</sub> is bound onto the GO surface.

The morphology of both the GO and GO–Fe<sub>3</sub>O<sub>4</sub> hybrid was characterized with TEM. The as prepared GO sheet is shown in Figure 1(A), which shows a clear edge contour. There is also some creased and twisted structure on the GO sheet. Compared with GO, it can be seen that some Fe<sub>3</sub>O<sub>4</sub> nanoparticles mainly exist on the edge of the GO sheet in GO–Fe<sub>3</sub>O<sub>4</sub> hybrid (Fig. 1(B)). The size of these nanoparticles is 2–4 nm with a narrow size distribution, and some Fe<sub>3</sub>O<sub>4</sub> aggregation is also observed. In this paper, Fe<sub>3</sub>O<sub>4</sub> nanoparticles are chemically deposited on GO with the aid of the –COOH on GO. The –COOH groups are mainly distributed on the edge of GO,<sup>15</sup> so we can see a preferential distribution of the nanoparticles on the edge of the GO sheet. Obviously, a large amount of Fe<sub>3</sub>O<sub>4</sub> nanoparticles are immobilized onto the GO sheets.

Figure 2 shows the XRD patterns of GO and GO–Fe<sub>3</sub>O<sub>4</sub> hybrid. The interlayer distance in the GO is about 0.8 nm, which is significantly larger than that of graphite, due to the intercalating oxide functional groups, such as epoxide and hydroxyl groups.<sup>16</sup> While in the GO–Fe<sub>3</sub>O<sub>4</sub> hybrid, this peak is shifted to 21.5°, indicating an interlayer distance of 0.4 nm. This can be explained by the partial removal the epoxide and the hydroxyl groups on GO, which were deoxygenated during Fe<sub>3</sub>O<sub>4</sub> nanoparticles deposition by treating with aqueous NaOH solution.<sup>17</sup> Another two new peaks are also observed in GO–Fe<sub>3</sub>O<sub>4</sub>

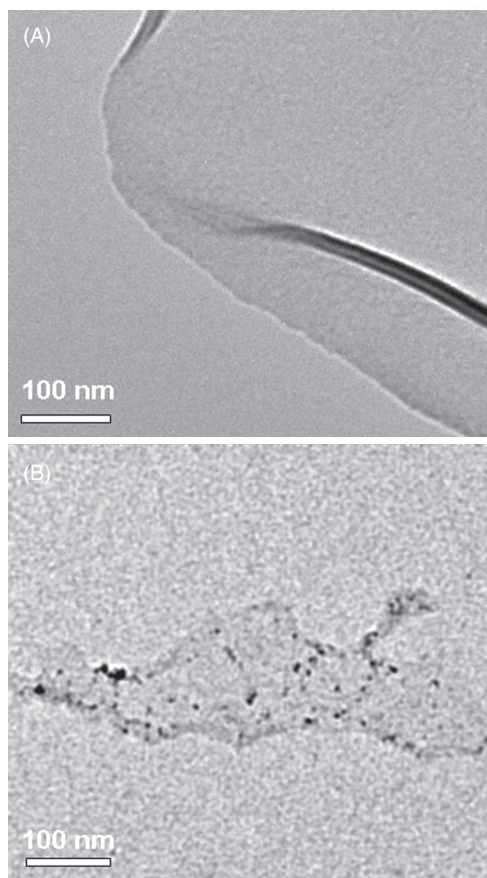


**Scheme 1.** Synthesis procedure of the GO-Fe<sub>3</sub>O<sub>4</sub> hybrid material.

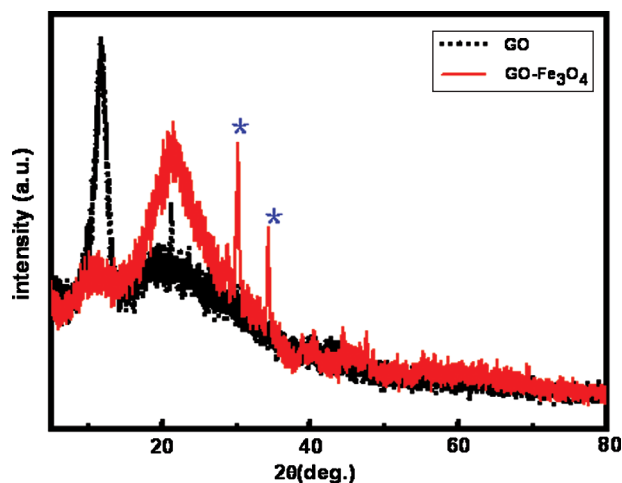
hybrid: 30.3° and 34.4°. These two peaks are the characteristic peaks of Fe<sub>3</sub>O<sub>4</sub>,<sup>18</sup> indicating that Fe<sub>3</sub>O<sub>4</sub> nanoparticles are loaded onto the GO sheets.

Figure 3 shows open-aperture Z-scan<sup>19</sup> results of GO, GO-Fe<sub>3</sub>O<sub>4</sub> and C<sub>60</sub>. The optical limiting properties of

the solutions of these materials were investigated using 532 nm pulsed laser irradiation, and C<sub>60</sub> was employed as a standard. To compare the optical limiting effect, all of the sample concentrations were adjusted to have same linear transmittance of 75% at 532 nm in 1-mm-thick cells. The open aperture Z-scan measures the transmittance of sample as it translates through the focal plane of a tightly focused beam. As the sample is brought closer to focus, the beam intensity increases and nonlinear effect increases, which will lead to a decreasing transmittance for reverse saturable absorption (RSA), two-photon absorption (TPA) and nonlinear scattering. As shown in Figure 3, the GO-Fe<sub>3</sub>O<sub>4</sub> shows the same dip with C<sub>60</sub>, which is much larger than GO. This indicates that GO-Fe<sub>3</sub>O<sub>4</sub> hybrid shows a much enhanced OL performance compared with GO and is comparable with the benchmark material-C<sub>60</sub>. Actually, during the measuring process, both of GO and GO-Fe<sub>3</sub>O<sub>4</sub>



**Fig. 1.** TEM images of GO (A) and GO-Fe<sub>3</sub>O<sub>4</sub> hybrid (B). The images were acquired from samples deposited onto a holey carbon support film.



**Fig. 2.** XRD patterns of GO (dotted line) and GO-Fe<sub>3</sub>O<sub>4</sub> hybrid (solid line). The two peaks (★) are the characteristic peaks of Fe<sub>3</sub>O<sub>4</sub>, indicating that Fe<sub>3</sub>O<sub>4</sub> nanoparticles are loaded onto the GO sheets.

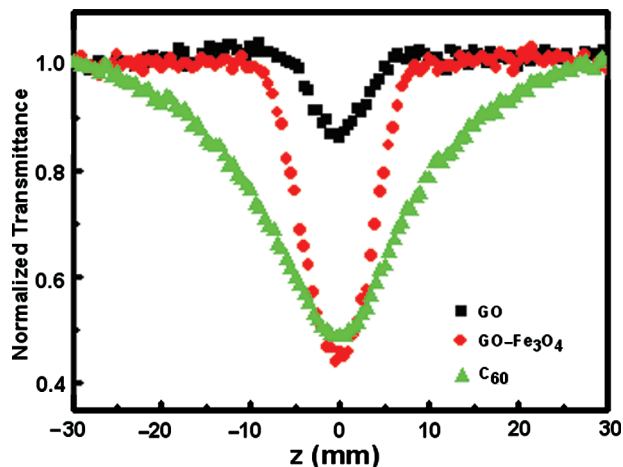


Fig. 3. Open aperture Z-scan results of GO(■), GO-Fe<sub>3</sub>O<sub>4</sub>(●) and C<sub>60</sub>(▲) with same linear transmittance of 75% to 5 ns, 532 nm optical pulses.

hybrid showed obvious nonlinear scattering signal, suggesting that nonlinear scattering plays an important role in these two samples. However, the nonlinear scattering signal of the GO-Fe<sub>3</sub>O<sub>4</sub> is much higher than GO. As can be seen from the TEM image of GO-Fe<sub>3</sub>O<sub>4</sub>, the size of Fe<sub>3</sub>O<sub>4</sub> nanoparticles is 2–4 nm. These nanoparticles are responsible for the enhancement of OL property due to the enhanced nonlinear scattering effect.

#### 4. CONCLUSION

In conclusion, the GO-Fe<sub>3</sub>O<sub>4</sub> hybrid material has been synthesized by a simple chemical deposition method and fully characterized. The formation of hybrid material was characterized by FTIR, TEM and XRD. The sizes of the Fe<sub>3</sub>O<sub>4</sub> nanoparticles on GO are mainly distributed between 2–4 nm. This hybrid material shows a much enhanced optical limiting performance compared with GO and is comparable with the benchmark material-C<sub>60</sub>. The mechanism responsible for the enhancement may be attributed to the enhanced nonlinear scattering effect introduced by the Fe<sub>3</sub>O<sub>4</sub> nanoparticles.

**Acknowledgment:** We gratefully acknowledge the financial support from the NSFC (#20774047), MoST (#2006CB932702) and NSF of Tianjin City (#07JCY-BJC03000, #08JCZDJC25300).

#### References and Notes

1. A. A. Balandin, S. Ghosh, W. Bao, I. Calizo, D. Teweldebrhan, F. Miao, and C. N. Lau, *Nano Lett.* 8, 902 (2008).
2. C. G. Lee, X. D. Wei, J. Kysar, and J. Hone, *Science* 321, 385 (2008).
3. K. I. Bolotin, K. J. Sikes, Z. Jiang, M. Klima, G. Fudenberg, J. Hone, P. Kim, and H. L. Stormer, *Solid State Commun.* 146, 351 (2008).
4. X. L. Li, X. R. Wang, L. Zhang, S. W. Lee, and H. J. Dai, *Science* 319, 1229 (2008).
5. X. Wang, L. Zhi, and K. Müllen, *Nano Lett.* 8, 323 (2008).
6. F. Schedin, A. K. Geim, S. V. Morozov, E. W. Hill, P. Blake, M. I. Katsnelson, and K. S. Novoselov, *Nat. Mater.* 6, 652 (2007).
7. Z. B. Liu, Y. Wang, X. L. Zhang, Y. F. Xu, Y. S. Chen, and J. G. Tian, *Appl. Phys. Lett.* 94, 21902 (2009).
8. Y. F. Xu, Z. B. Liu, X. L. Zhang, Y. Wang, J. G. Tian, Y. Huang, Y. F. Ma, X. Y. Zhang, and Y. S. Chen, *Adv. Mater.* 21, 1275 (2009).
9. C. P. Singh, K. S. Bindra, G. M. Bhalerao, and S. M. Oak, *Opt. Express* 16, 8440 (2008).
10. K. C. Chin, A. Gohel, W. Z. Chen, H. I. Elim, W. Ji, G. L. Chong, C. H. Sow, and A. T. S. Wee, *Chem. Phys. Lett.* 409, 85 (2005).
11. W. S. Hummers and R. E. Offeman, *J. Am. Chem. Soc.* 80, 1339 (1958).
12. H. A. Becerril, J. Mao, Z. F. Liu, R. M. Stoltenberg, Z. N. Bao, and Y. S. Chen, *ACS Nano* 2, 463 (2008).
13. X. Y. Yang, X. Y. Zhang, Y. F. Ma, Y. Huang, Y. S. Wang, and Y. S. Chen, *J. Mater. Chem.* 19, 2710 (2009).
14. S. F. Chin, K. S. Iyer, and C. L. Raston, *Lab on a Chip* 8, 439 (2008).
15. A. Lerf, H. Y. He, M. Forster, and J. Klinowski, *J. Phys. Chem. B* 102, 4477 (1998).
16. M. J. McAllister, J. L. Li, D. H. Adamson, H. C. Schniepp, A. A. Abdala, J. Liu, M. Herrera-Alonso, D. L. Milius, R. Car, R. K. Prud'homme, and I. A. Aksay, *Chem. Mater.* 19, 4396 (2007).
17. X. B. Fan, W. C. Peng, Y. Li, X. Y. Li, S. L. Wang, G. L. Zhang, and F. B. Zhang, *Adv. Mater.* 20, 4490 (2008).
18. R. A. Silva, M. J. L. Santos, A. W. Rinaldi, A. J. G. Zarbin, M. M. Oliveira, I. A. Santos, L. F. Cotica, A. A. Coellho, A. F. Rubira, and E. M. Giroto, *J. Solid State Chem.* 180, 3545 (2007).
19. M. Sheik-Bahae, A. A. Said, T. H. Wei, D. J. Hagan, and E. W. Van Stryland, *IEEE J. Quantum Electron.* 26, 760 (1990).

Received: 11 June 2009. Accepted: 16 June 2009.